

# Technical Report of SWAMP NGC

Massimo Caccia, Marco Bibuli, Gabriele Bruzzone,  
Enrica Zereik, Angelo Odetti

September 2020

## 1 Navigation Guidance and Control

Single vehicle NGC system, both as catamaran or single hull vessel, consists of a dual-loop hierarchical guidance and control architecture of the class presented in [1]. As shown in Figure 1, the outer guidance loop manages the kinemat-

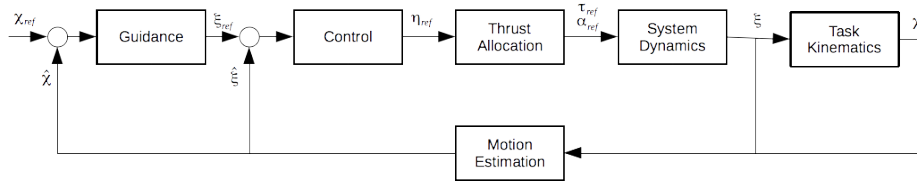


Figure 1: Navigation Guidance and Control architecture

ics interactions between the vehicle and the environment at task function level and generates the reference linear and angular velocities for the control module. The inner control loop handles system dynamics, implementing a velocity servo-loop for surge, sway, yaw respectively, to generate the desired surge and sway forces and yaw torque. Motion estimation is based on (partial) knowledge of system dynamics and extended Kalman filtering techniques, as discussed in [2], where basic guidance and control algorithms, including straight line-following, are presented. Advanced techniques for generic path-following and multi-vehicle cooperative guidance, e.g. vehicle-following, are presented in [3] and [4], respectively.

Thanks to NGC system modularity, it is only needed to tune parameters of the guidance, control and motion estimation algorithms and to design and implement the Thrust Allocation module, that is specific of each vessel class.

### 1.1 Thrust allocation

Each Pump-Jet Module is constituted by two motors:

- **Azimuth motor** controlling the orientation  $\alpha_i$  of the thrust exerted by the  $i$ -th jet, assumed equal to 0 when the thruster pushes along the surge direction. For simulation purposes, the controlled motor can be assumed to have a first-order dynamics with time constant  $t_\alpha$ , i.e.  $\frac{1}{1+t_\alpha s}$
- **Pump motor** controlling the thrust  $T_i^{PJ}$  exerted by the  $i$ -th jet. The pump motor is assumed to have time constant equal to zero. Each Pump-Jet is positioned at  $\underline{p}_i^{PJ} = [l_i^{PJ}, b_i^{PJ}, 0]^T$  with rotation matrix  $R_{PJ_i,b} = I$  with respect to the vehicle-fixed reference frame  $\langle b \rangle$ . The resulting rotation matrix between the Pump-Jet thrust and the vehicle-fixed reference frame is

$$\begin{bmatrix} \cos \alpha_i & -\sin \alpha_i & 0 \\ \sin \alpha_i & \cos \alpha_i & 0 \\ 0 & 0 & 0 \end{bmatrix} \quad (1)$$

The contribution to the external force and torque given by each Pump-Jet is:

$$\underline{\tau}^{PJ} = \begin{bmatrix} X_i^{PJ} \\ Y_i^{PJ} \\ N_i^{PJ} \end{bmatrix} = \begin{bmatrix} \cos \alpha_i \\ \sin \alpha_i \\ -b_i^{PJ} \cos \alpha_i + l_i^{PJ} \sin \alpha_i \end{bmatrix} T_i \quad (2)$$

## 1.2 Generic thrust allocation algorithm

Referring to [5], in the case of SWAMP ASV, denoting with

$$\begin{aligned} X_i^{PJ} &= T_i \cos \alpha_i \\ Y_i^{PJ} &= T_i \sin \alpha_i \\ i &= 1..4 \end{aligned} \quad (3)$$

the extended thrust vector  $\underline{T}_{ext}^{PJ}$  is defined as

$$\underline{T}^{PJ} = [X_1^{PJ} Y_1^{PJ} X_2^{PJ} Y_2^{PJ} X_3^{PJ} Y_3^{PJ} X_4^{PJ} Y_4^{PJ}]^T \quad (4)$$

and the generalised force for the Pump-Jet system is computed as

$$\underline{\tau}^{PJ} = B \underline{T}^{PJ} \quad (5)$$

where

$$B = \begin{bmatrix} 1 & 0 & 1 & 0 & 1 & 0 & 1 & 0 \\ 0 & 1 & 0 & 1 & 0 & 1 & 0 & 1 \\ b_1^{PJ} & l_1^{PJ} & b_2^{PJ} & -l_2^{PJ} & -b_3^{PJ} & l_3^{PJ} & -b_4^{PJ} & -l_4^{PJ} \end{bmatrix} \quad (6)$$

Each Pump-Jet thrust is assumed to be positive and lower than a maximum

value as it follows

$$\begin{aligned}
X_i^{PJ} \cos \alpha_i + Y_i^{PJ} \sin \alpha_i &\leq T_i^{MAX} \\
X_i^{PJ} \cos \alpha_i + Y_i^{PJ} \sin \alpha_i &\geq T_i^{min} \\
\alpha_i &= \text{atan2}(Y_i^{PJ}, X_i^{PJ}) \\
i &= 1..4
\end{aligned} \tag{7}$$

Being  $\alpha_{i,0}$  the current orientation of the  $i$ -th Pump-Jet and  $\Delta\alpha$  the maximal angle variation in the sampling period, the following Angular sector constraint(s)-rotation rate constraint(s) hold:

$$\begin{cases} X_i^{PJ} \sin(\alpha_{i,0} - \Delta\alpha) - Y_i^{PJ} \cos(\alpha_{i,0} - \Delta\alpha) \leq 0 \\ -X_i^{PJ} \sin(\alpha_{i,0} + \Delta\alpha) + Y_i^{PJ} \cos(\alpha_{i,0} + \Delta\alpha) \geq 0 \end{cases} \quad i = 1..4 \tag{8}$$

The general DP-TA problem can be summarised as minimising a cost function including a quadratic approximation of the power consumption as well as a penalty for variations in the extended thrust vector that is intended to reduce wear-and-tear in the thrusters. The study of ad-hoc optimisation also considering hydrodynamic effects of pumpjet-hull interactions at different operating speed will be the subject of further research. In the initial validation and development phase of the prototype vehicle a practical approach, based on the implementation of conventional thrust allocation schemes in specific operational configurations, was followed.

### 1.3 Thrust allocation in selected working configurations

Specific Pump-Jet configurations are selected corresponding to typical working modes such as, for instance, *station-keeping* and *forward/backward surge transfer*. In these cases, the Pump-Jet orientation angles are constrained in pre-defined sectors and, according to the positive thrust physical constraint, suitable sub-sets of actuators are allocated to generate the desired directional force and torque.

#### 1.3.1 Station-Keeping thrust allocation

In the case of station-keeping Pump-Jet are symmetrically positioned in order to generate force and torque in any direction at any time, as shown in Figure 2. The Pump-Jet orientation angle  $\alpha$  is such that  $\alpha \in (0, \frac{\pi}{2})$ , while  $d_i^{PJ}$  and  $l_i^{PJ}$  are assumed to be equal to  $d$  and  $l$  respectively for  $i = 0..3$ .

The requested thrust  $T_i$  for each Pump-Jet is computed, given a fixed  $\alpha$ , as superposition of the actions generating the desired force and torque  $[X, Y, N]^T$ :

$$T_i(X, Y, N, \alpha) = T_i(X, \alpha) + T_i(Y, \alpha) + T_i(N, \alpha) \tag{9}$$

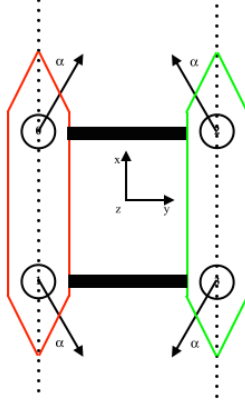


Figure 2: Station-Keeping Pump-Jet configuration

Force and torque are mapped on Pump-Jet according to X, Y, and N signs as reported in the following:

- surge force is mapped on bow and stern pump-jets when directed forward and backward respectively

$$T_0(X, \alpha) = T_2(X, \alpha) = \begin{cases} \frac{X}{2 \cos \alpha} & , X > 0 \\ 0 & , X < 0 \end{cases}$$

$$T_1(X, \alpha) = T_3(X, \alpha) = \begin{cases} 0 & , X > 0 \\ -\frac{X}{2 \cos \alpha} & , X < 0 \end{cases}$$

- sway force is mapped on port and starboard pump-jets when directed starboard and port respectively

$$T_0(Y, \alpha) = T_1(Y, \alpha) = \begin{cases} \frac{Y}{2 \sin \alpha} & , Y > 0 \\ 0 & , Y < 0 \end{cases}$$

$$T_2(Y, \alpha) = T_3(Y, \alpha) = \begin{cases} 0 & , Y > 0 \\ -\frac{Y}{2 \sin \alpha} & , Y < 0 \end{cases}$$

- yaw torque is mapped on opposite diagonal pump-jets

$$T_0(N, \alpha) = T_3(N, \alpha) = \begin{cases} \frac{N}{2(d \cos \alpha + l \sin \alpha)} & , N > 0 \\ 0 & , N < 0 \end{cases}$$

$$T_1(N, \alpha) = T_2(N, \alpha) = \begin{cases} 0 & , N > 0 \\ -\frac{N}{2(d \cos \alpha + l \sin \alpha)} & , N < 0 \end{cases}$$

Then  $\alpha$  is selected such that

$$\alpha : \min_{\alpha \in (0, \frac{\pi}{2})} \sum_{i=0}^3 T_i^2(X, Y, N, \alpha) \quad (10)$$

### 1.3.2 Surge-Forward thrust allocation

In the case of surge-forward working mode, surge and sway force are assumed to be positive and zero respectively, while pump-jets are symmetrically positioned in order to generate yaw torque in any direction at any time, as shown in Figure 3.

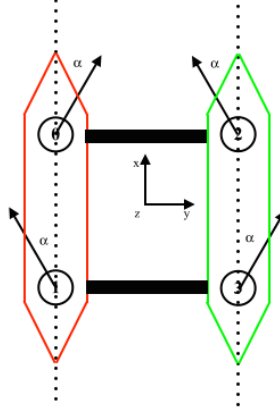


Figure 3: Surge-Forward pump-jet configuration

Surge force and yaw torque are mapped on pump-jets according to  $N$  sign as reported in the following:

- Surge force is equally distributed on the four pump-jets

$$T_i(X, \alpha) = \frac{X}{4 \cos \alpha}, \quad i = 0..3$$

- Yaw torque is mapped on port and starboard pump-jets

$$T_0(N, \alpha) = T_1(N, \alpha) = \begin{cases} \frac{N}{2(b \cos \alpha + l \sin \alpha)} & , N > 0 \\ 0 & , N < 0 \end{cases}$$

$$T_2(N, \alpha) = T_3(N, \alpha) = \begin{cases} 0 & , N > 0 \\ -\frac{N}{2(b \cos \alpha + l \sin \alpha)} & , N < 0 \end{cases}$$

## 1.4 Single hull vessel

A SWAMP single hull vessel is equipped with a bow and a stern pump-jet with thrust and orientation  $(T_B, \alpha_B)$  and  $(T_S, \alpha_S)$  respectively.

Denoting with

$$A = \begin{bmatrix} \cos \alpha_B & \cos \alpha_S \\ \sin \alpha_B & \sin \alpha_S \\ \sin \alpha_B & -\sin \alpha_S \end{bmatrix} \quad (11)$$

$$\mathbf{b} = \begin{bmatrix} X \\ Y \\ \frac{N}{l} \end{bmatrix} \quad (12)$$

$$\mathbf{x} = \begin{bmatrix} T_B \\ T_S \end{bmatrix} \quad (13)$$

the resulting force and torque are

$$\mathbf{b} = A\mathbf{x} \quad (14)$$

Given  $\alpha_B$  and  $\alpha_S$  and the desired force and torque, a solution to 14 is provided by LS and Moore-Penrose pseudo-inverse

$$\hat{\mathbf{x}} = (A^T A)^{-1} A^T \mathbf{b} \quad (15)$$

where

$$A^T A = \begin{bmatrix} \cos^2 \alpha_B + 2 \sin^2 \alpha_B & \cos \alpha_B \cos \alpha_S \\ \cos \alpha_B \cos \alpha_S & \cos^2 \alpha_S + 2 \sin^2 \alpha_S \end{bmatrix} \quad (16)$$

Note: the constraint  $0 \leq T_B, T_S \leq T_{MAX}$  must be satisfied.

## References

- [1] M. Caccia and G. Veruggio. Guidance and control of a reconfigurable unmanned underwater vehicle. *Control Engineering Practice*, 8(1):21–37, 2000.
- [2] M. Caccia, M. Bibuli, R. Bono, and G. Bruzzone. Basic navigation, guidance and control of an unmanned surface vehicle. *Autonomous Robots*, 25(4):349–365, 2008.
- [3] Marco Bibuli, Gabriele Bruzzone, Massimo Caccia, and Lionel Lapierre. Path-following algorithms and experiments for an unmanned surface vehicle. *Journal of Field Robotics*, 26(8):669–688, 2008.
- [4] Marco Bibuli, Massimo Caccia, Gabriele Bruzzone, and Lionel Lapierre. Guidance of unmanned surface vehicles: Experiments in vehicle following. *IEEE Robotics and Automation Magazine*, 19(3):92–102, 2008.
- [5] A. Veksler, T.A. Johansen, F. Borrelli, and B. Realfsen. Cartesian thrust allocation algorithm with variable direction thrusters, turn rate limits and singularity avoidance. In *2014 IEEE Conference on Control Applications (CCA)*, pages 917–922. IEEE, 2014.